

1

2 **Original Research Article**

3 **Warming Effect Reanalysis of Greenhouse**

4 **Gases and Clouds**

5 **ABSTRACT**

6

The author has reanalysed the warming effects of greenhouse (GH) gases utilising the latest HITRAN 2012 database and improved water continuum calculations in the spectral analysis tool. The contributions of GH gases in the GH effect in the all-sky conditions are found to be: H₂O 81 %, CO₂ 13 %, O₃ 4 %, CH₄ & N₂O 1 %, and clouds 1 %. Because the total absorption is already 93 % from the maximum in the altitude of 1.6 km, which is the average global cloud base, the GH gas impacts are almost the same in the clear and all-sky conditions. The impacts of clouds are based on the normal cloudiness changes between the clear and cloudy skies. The positive impact of clouds is analysed and it is based on the warming impact of clouds during the night-time. The warming impact of CO₂ is very nonlinear and it means that in the present climate the strength of H₂O is 11.8 times stronger than CO₂, when in the total GH effect this relationship is 6.2:1. The atmospheric Total Precipitable Water (TPW) changes during ENSO events are the essential parts of the ENSO process and they are not actually separate feedback processes. The TPW changes during the ENSO events almost double the original ENSO effects. On the other hand, during Mt. Pinatubo eruption and during the three latest solar cycles, the long-term water feedback effect cannot be found despite of rapid warming from 1980 to 2000. This empirical result confirms that the assumption of no water feedback in calculating the climate sensitivity of 0.6 °C is justified. Because there is no long-term positive feedback, it explains why the IPCC model calculated temperature 1.2 °C in 2015 is 44 % greater than the average 0.85 °C of the pause period since 2000.

7

8 *Keywords: Global warming; greenhouse effect; greenhouse gases; climate sensitivity; cloud*

9 *forcing; water feedback*

10

11

12
13
14
15
16
17
18
19
20
21
22
23
24
25
26
27
28
29
30
31
32
33
34

1. INTRODUCTION

1.1 Objectives and Symbols

The physical properties of greenhouse (GH) gases in absorbing shortwave and longwave radiation have been well-known for decades. The latest updated knowledge has not been always available in some common spectral analysis tools. This has been also the case with the Spectral Calculator [1], the tool used by the author in earlier analyses. Now the latest HITRAN line data version 2012 is available [2]. The coefficients in water continuum model are also updated as to 2.5.2 MT_CK [3].

These updates created an objective to reanalyse the warming impacts of GH gases in the GH phenomenon itself and the real impacts in the present climate. The warming and cooling effects of clouds have been a continuous issue of different opinions and therefore it is another objective of this study. The third objective is to carry out a water feedback analysis, which has a major impact on the climate sensitivity (CS).

Table 1 includes all the symbols, abbreviations, acronyms, and definitions used repeatedly in this paper.

Table 1. List of symbols, abbreviations, and acronyms

Acronym	Definition
AGA	Average Global Atmosphere
CS	Climate Sensitivity
CSP	Climate Sensitivity Parameter ($=\lambda$)
ENSO	El Niño Southern Oscillation
GCM	General Circulation Model
LW	Longwave
MLS	Mid-latitude climate zone, summer
MLW	Mid-latitude climate zone, winter
OLR	Outgoing longwave radiation
prcm	precipitated water in centimetre
PS	Polar climate zone, summer
PW	Polar climate zone, winter
RF	Radiative Forcing change
SW	Shortwave
TCF	Temporary Climate Forcing
TOA	Top of the Atmosphere
TPW	Total Precipitable Water
TROP	Tropical climate zone
UAH	University of Alabama in Huntsville temperature data set

35
36
37
38
39
40
41
42
43
44

1.2 The Survey of Greenhouse Effect Studies

The difference between the average global mean surface temperature (15°C) and the temperature (-19°C) corresponding to the average outgoing longwave (LW) radiation (239 Wm^{-2}) at the top of the atmosphere (TOA) is a common measure of terrestrial GH effect thus being 34°C . The GH gases and clouds absorb the LW radiation emitted by the Earth's surface and in this way, they prevent the cooling of the Earth making it a habitable planet.

45 The number of studies for calculating and analyzing the contributions of GH gases is
 46 surprisingly low. The most important results are summarized in Table 2.

47
 48
 49
 50

Table 2. The contribution percentages of GH gases in the GH phenomenon after different studies.

GH gas	Michell	Kiehl & Trenberth	Schmidt et al.	Ollila
H ₂ O	65	60 (38)	50	82
CO ₂	32	26	19	11
O ₃	1	8	Others 7	5
CH ₄ & N ₂ O	2	6		2
Clouds		(39)	25	

51
 52

53 Michell [4], Kiehl & Trenberth [5], and Ollila [6] have carried out the calculations in the clear
 54 sky conditions and Schmidt et al (7) values are for all-sky. Kiehl & Trenberth have also two
 55 percentages for cloudy sky conditions. In addition to these comprehensive studies, there are
 56 some studies indicating percentages for individual GH gases: Clough et lacono [8] water 63
 57 %, Miskolczi & Mlynczak [9] CO₂ 9 % and Pierrehumbert [10] CO₂ about 33 %.

58

59 The atmosphere composition applied in the calculations has a decisive role. Michell has not
 60 specified the atmosphere. Kiehl & Trenberth have used US Standard 76 atmosphere (USST
 61 76) and they have reduced the water content by 12 %. It means that in their analysis, the
 62 water content is only 50 % about the average global atmosphere (AGA), which is 2.6 prcm
 63 (precipated water in centimeters). Ollila [11] has carried out these calculations also applying
 64 the USST 76 and the results are very close to Kiehl & Trenberth [5]. Even though some
 65 researchers [12] think that the use of USST 76 is an international and IPCC accepted
 66 standard for atmospheric calculations, its composition makes it not applicable for any global
 67 atmospheric calculations.

68

69 The calculation method is not similar in all studies. Kiehl & Trenberth [5], Miskolczi &
 70 Mlynczak [9] and Ollila [11] have calculated the contribution of each GH gas by removing it
 71 from the atmospheric model. Schmidt et al. [7] have used a more complicated method by
 72 calculating the minimum and maximum impact. The minimum impact comes from the
 73 removing process and the maximum by applying the GH gas in question alone in the
 74 atmosphere. In this case, the result concerning the major absorbers water, carbon dioxide
 75 and clouds is almost exactly the average value of minimum and maximum impacts.

76

77 Only Schmidt et al. [7] have proposed that clouds have a positive contribution in the GH
 78 phenomenon even though they admit that the net radiative impact including SW effects of
 79 clouds is one of cooling. This is one of the issues discussed and analyzed later in this study.

80

81 The spread of the results in the contributions of GH gas may have been a reason, why IPCC
 82 has not concluded what are the most reliable values.

83

84

85 **2. ABSORPTION BY GREENHOUSE GASES**

86

87 **2.1 Effects of HITRAN 2012 and Water Continuum**

88

89 The first calculations were carried out to find out the impacts of HITRAN 2012 and water
 90 continuum updates in the absorption calculations. The author has used in earlier studies the

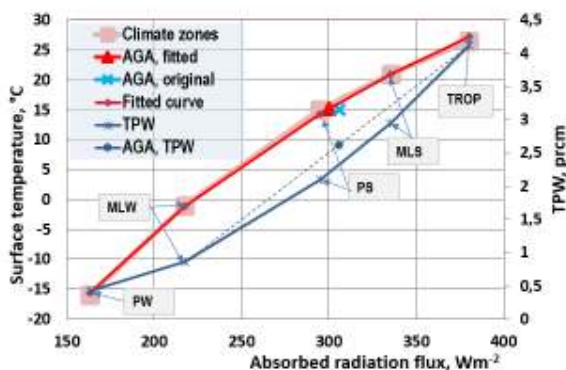
91 atmospheric one profile model called average global atmosphere (AGA) [6], [11], [13], [14],
 92 [15], [16], [17]. This model was based on the GH gas concentrations in 2005 and therefore it
 93 is called AGA05. The GH gas concentrations of AGA05 are modified from the GH gas
 94 profiles of the Polar Summer of Spectral Calculator to correspond the values reported by
 95 IPCC [18]. The water profile was adjusted in such a way that the total precipitable water
 96 (TPW) was 2.6 cm [19].

97
 98 The total absorption in the troposphere applying the AGA05 condition and the HITRAN 2008
 99 version was 302.709 Wm^{-2} . When the AGA05 was applied using the newest HITRAN 2012
 100 version and the updated water continuum, the total absorption was 303.308 Wm^{-2} . It is only
 101 a 0.2 % greater value, which mean that these updates have a very small effect for
 102 absorption calculations.

103
 104 In later calculations of this study, the GH gas concentrations are updated to correspond with
 105 the values in year 2015 [20] and therefore this climate model is called AGA15. The AGA15
 106 profile gives the value of 305.978 Wm^{-2} as the total absorption. The difference is mainly due
 107 to the higher CO_2 concentration (400.83 ppm versus 379 ppm).

109 2.2 Simulation of Climate Zones

110
 111 I have used one climate profile in calculations utilizing AGA15. Because the climate varies in
 112 the different climate zones, the question is, how well one profile represents the global
 113 conditions. This can be tested by calculating the absorption in the troposphere applying 5
 114 climate zones: tropical (TROP), mid-latitude summer (MLS), mid-latitude winter (MLW), polar
 115 summer (PS) and polar winter (PW). The results of these calculations are (Wm^{-2}): PW
 116 163.329, PS 294.701, MLW 217.534, MLS 335.221, and TROP 380.064. Utilizing the
 117 weighting factor based on the geographical areas for these climate zones [19], the global
 118 absorption value is 307.533 Wm^{-2} . It is only 0.5 % higher than 305.978 Wm^{-2} calculated
 119 applying the one profile approach AGA15. The difference is mainly due to the fact that the
 120 TPW value of climate zones is 2.7 cm and the one of AGA15 is 2.6 cm. The results of these
 121 calculations are depicted in Figure 1.



123
 124
 125 **Figure 1. The relationship between the absorption fluxes, temperatures, and water**
 126 **contents of different climate zones. The climate zones of the curves starting from the**
 127 **left corner are PW, MLW, PS, MLS, TROP. The temperatures and TPW values are from**
 128 **the climate profiles of Spectral Calculator [1].**

129
 130 The relationship between the temperatures (T , $^{\circ}\text{C}$) and absorption energies (E , Wm^{-2}) is
 131 logarithmic:

132

$$T = -274.3249 + 50.7558 * \ln(E) \quad (1)$$

133

134

135 The coefficient of determination r^2 is 0.999 and the standard error of the temperature
 136 estimate is 0.9 °C. In Fig.1 is depicted also the AGA15 value, which is 15 °C / 305.978 Wm⁻².
 137 This point is not exactly on the fitting curve, because the overall TPW value of climate zones
 138 is 2.7 cm and the one of AGA15 is 2.6 cm. The AGA15 point (a blue cross) is slightly
 139 modified to fit it (a red triangle) on the curve applying the values of 15.19 °C / 300 Wm⁻².
 140 The blue curve shows the increasing TPW values according to the warmer climate zones.
 141 The blue dot is the AGA15 value of 2.6 prcm.

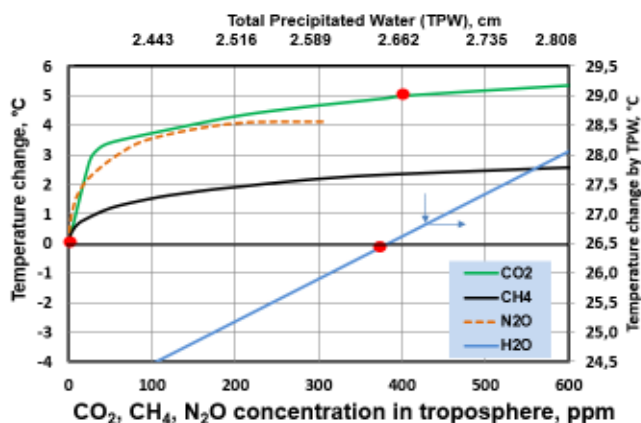
142

143 2.3 Warming Impacts of Greenhouse Gases in the Clear Sky

144

145 Applying the AGA15 atmospheric profile, the absorption values of GH gases can be
 146 calculated by changing the concentration of each GH gas starting from zero level in clear sky
 147 condition. The warming effects can be then calculated by using equation (1). The results are
 148 depicted in Fig. 2.

149



150

151

152 **Fig. 2. The warming impacts of GH gases in the clear sky conditions. The red dots**
 153 **represent the concentrations and warming impacts of the year 2015.**

154

155 The warming effect of CO₂ is highly nonlinear in the present atmosphere but the effect of
 156 H₂O is practically linear around the average TPW value of 2.6 cm. Also, the concentrations
 157 of CH₄ and N₂O are so low that they are still in the region of Beer-Lambert law, where the
 158 absorption is almost linearly dependent on the gas concentration. The warming impacts of
 159 CO₂ can be fitted with the logarithmic equation:

160

$$T = -1.01403 + 0.988487 * \ln(\text{CO}_2) \quad (2)$$

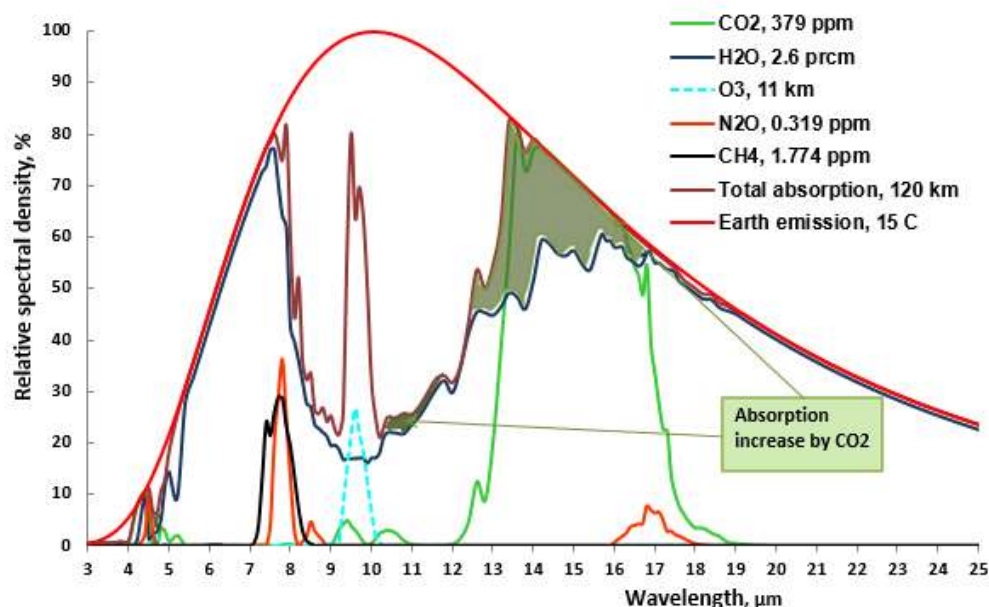
162

163 where T is the temperature impact (°C) and CO₂ is the concentration of CO₂ (ppm). The
 164 coefficient of determination r^2 is 0.999, the standard error is 0.02 °C. This formula is valid in
 165 the concentration range from 200 ppm to 800 ppm. This formula gives the temperature
 166 change 0.6 °C for the CO₂ concentration from 280 ppm to 560 ppm.

167

168 The reasons for the nonlinear effects can be illustrated by the absorption graphs of GH
 169 gases, when the relative spectral density is calculated as a function of wavelength. In Fig. 3
 170 the absorption graphs are depicted from the 3 μm to 25 μm.

171



172
173
174
175
176
Figure 3. The absorption band Graphs of GH gases in the AGA05 atmosphere. The green shaded areas indicate a total warming impact of CO₂ of concentration of 379 ppm.

177 Water absorbs completely all the IR radiation emitted by the Earth's surface in the
178 wavelength zone from 25 μm to 100 μm. The shaded green area gives a good image of the
179 magnitude of CO₂. The absorption area changes due to the increased concentrations of
180 CO₂, CH₄, and N₂O from 2005 to 2015 are so small that they could not be detected in the
181 graphical presentation of Fig. 3.

182
183 The curve of each GH gas is calculated when it is the only GH gas in the atmosphere in the
184 AGA05 conditions. The combined effect of all GH gases is not a summary of the band areas
185 of single GH gases. The actual total absorption can be calculated only when all the GH
186 gases are present at the same time. The total absorption is depicted by the purple line. The
187 absorption areas of CH₄ and N₂O show that they are very small and inside the absorption
188 areas of H₂O, which reduces their impacts further. Also, the CO₂ absorption area overlaps
189 with water and the real impacts are possible to calculate only by the means of spectral
190 analysis by varying the CO₂ concentration.

191 192 **3. WATER FEEDBACK**

193 194 **3.1 Water Feedback in the Climate Zones**

195
196 Water feedback is one of the most important issues in the climate change science. The
197 results and opinion deviate completely from each other. IPCC and many research
198 communities use the approach that water feedback exists and it is positive in nature by
199 doubling the warming effects of other GH gases. The Table 9.5 in AR5 [21] summarizes 30
200 different GCMs (General Circulation Model), which have the Climate Sensitivity Parameter
201 (CSP or λ) averaging 1.0 K/(Wm⁻²). Because this CSP value is for Equilibrium Climate
202 Sensitivity (ECS) value, it includes water feedback and other positive feedbacks. The CSP
203 value of 0.5 K/(Wm⁻²) includes only water feedback [21]. The opposite result is from

204 Miskolczi [19] that the GH effect of the Earth's climate is constant, which means that the
 205 water feedback is negatively compensating for the warming effects of other GH gases.

206

207 One possible way to analyze the water feedback is to calculate the warming effect of water
 208 by hypothesizing that the Earth's climate follows the humidity features of the climate zones.
 209 From Fig. 1 it is easy to find out that the absolute water content increases as the climate is
 210 getting warmer.

211

212 The absorption flux of CO₂ concentration 280 ppm is 298.728 Wm⁻² and the same of CO₂
 213 concentration 560 ppm is 301.177 Wm⁻², which corresponds the temperature change of 0.48
 214 °C according to equation (1). If we assume that the absolute water content of the global
 215 atmosphere follows the climate zone behavior, the water content change would increase this
 216 absorption change like this: 280 ppm absorption 297.728 Wm⁻² and 560 ppm absorption
 217 301.592 Wm⁻². This change corresponds to the temperature change 0.66 °C. Thus, the
 218 water feedback would positively increase the warming effects of GH gases by 35.4 %.

219

220 **3.2 Water Feedback During the Last 25 Years**

221

222 Rather reliable conclusions about the water feedback can be drawn from the behavior of the
 223 climate during the last 35 years. I have selected this period, because the encompassing
 224 satellite temperature measurements were introduced in 1979. Also, a new humidity
 225 semiconductor sensor technology Humicap® was introduced by the leading humidity
 226 measurement company Vaisala. This technology replaced rapidly the hygrometer
 227 technology, because it was more accurate and more reliable than the hygrometer
 228 technology.

229

230 I have started the analysis from the year 1979 by modifying temperature changes and all
 231 warming impacts to start from zero. The temperature is according to the UAH satellite data
 232 set [22] and absolute TPW values from NOAA [23] NCEP/NCAR Reanalysis dataset. The
 233 warming impacts of water are calculated based on the absorption calculations by increasing
 234 the water content of the AGA conditions (2.6 prcm / 305.978 Wm⁻²) to the TPW value of
 235 2.856 prcm giving the absorption value of 306.709 Wm⁻². By forcing the warming value (T) in
 236 Celcius degrees to be zero in 1979, equation (3) could be concluded:

237

$$238 \quad T = -6.797 + 2.81 * TPW, \quad (3)$$

239

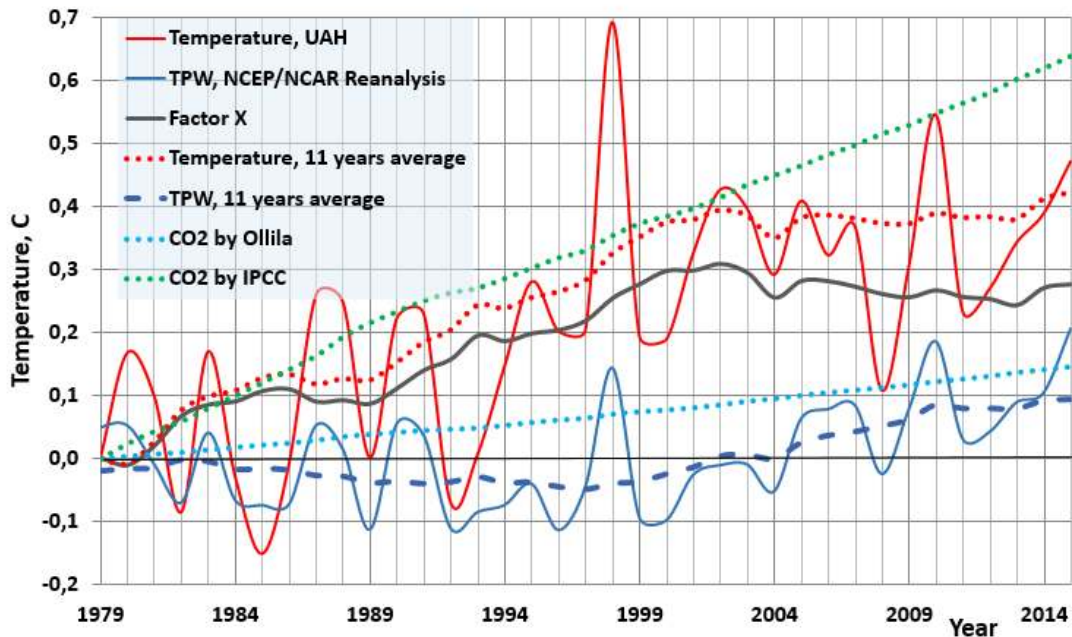
240 where TPW is the absolute humidity in prcm. The warming impact of CO₂ is calculated by
 241 the equation introduced by Ollila [6]:

242

$$243 \quad T = CSP * k * \ln(C/280), \quad (4)$$

244

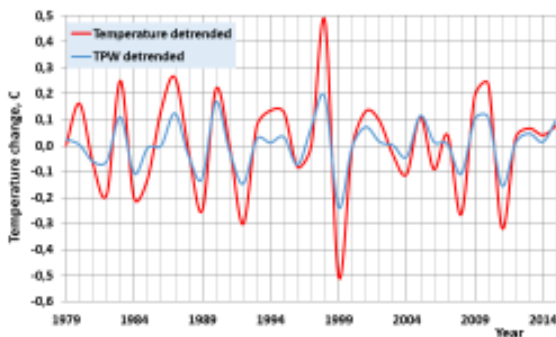
245 where CSP is 0.27 K/(Wm⁻²), and k is 3.12 in the formula of radiative forcing of CO₂ (Wm⁻²).
 246 The CO₂ concentration changes are from the data set of NOAA [20]. The results of these
 247 calculations are depicted in Fig. 4.



248
249
250
251
252
253
254
255
256
257
258
259
260
261
262
263

Figure 4. The temperature trend from according to UAH [22] and the major warming factors, which are absolute humidity and CO₂. The variable labelled “Factor X” is the difference between the measured average temperature and the warming impacts of CO₂ by Ollila [6]. El Niño events are marked as to the strengths and they are followed by La Niña events which are not marked.

The variable labelled “Factor X” is also depicted in Fig. 4. It is the difference between the measured average 11 years temperature and the warming effect of CO₂ by Ollila [6]. This presentation makes it very clear that the warming impacts of water, CO₂, and ENSO events cannot explain the observed warming. It is easy to notice that the short-term temperature changes very closely correlated to the TPW changes. This relationship is even easier to notice from Fig. 5, where these two variables are detrended. All the short-term changes are ENSO events except Mt. Pinatubo eruption in 1991.



264
265
266
267
268

Figure 5. The detrended graphs of temperature and TPW values.

A hasty conclusion would be that the TPW variations have caused the temperature changes since 1979 until today. Looking at the shape of the monotonically rising temperature effect of

269 CO₂ (IPCC or Ollila) and the sharp short-term changes of TPW, it is very clear that the
270 relationship between these two variables is very poor.

271

272 The detrended analysis reveals that the short-term TPW changes could explain about 50 %
273 of the short-term temperature changes. Concerning the El Niño / La Niña events, we already
274 know that the cause is the regional changes in Pacific Ocean currents and winds. They
275 initiate the temperature change and the strong change of TPW amplifies the change by a
276 factor of about 100 percent. It is practically the same as the positive feedback used by IPCC,
277 but can it be found in the long-term trends?
278

279 There is an essential feature in the long-term trends of temperature and TPW, which are
280 calculated and depicted as 11 years running mean values. The long-term value of
281 temperature has increased about 0.4 °C since 1979 and it has now paused to this level. The
282 long-term trend of TPW shows a minor decrease of 0.05 °C during the temperature
283 increasing period from 1979 to 2000 and thereafter only a small increase of 0.08 °C during
284 the present temperature pause period. It means that the absolute water amount of the
285 atmosphere is practically constant reacting only very slightly to the long-term trends of
286 temperature changes. Long-term changes, which last at least one solar cycle (from 10.5 to
287 13.5 years), are the shortest period to be analyzed in the climate change science. The
288 assumption that the relative humidity is constant and it amplifies the GH gas changes by
289 doubling the warming effects, finds no grounds based on the behavior of TWP trend.
290

291 It seems that there is a dilemma between the short-term behavior of TPW changes and the
292 long-term (> 11 years) changes. It looks like that the global atmosphere does not behave in
293 the same way as it does in the climate zones, where a higher temperature means always a
294 higher TWP value. Because the analysis period is slightly more than three solar cycles, the
295 conclusions for long-term behavior of TPW is rather reliable. This result supports the climate
296 sensitivity (CS) calculations, where the absolute water amount has been assumed to be
297 constant, and which gives the CS value of 0.6 °C [6].
298

299 So, there is a "Factor X", the unknown force or forces that change the Earth's temperature.
300 During the period from 1995 to 2005 these forces have caused a temperature increase of a
301 0.2-0.3 °C and now these effects are decreasing, see the black curve in Fig. 4. These forces
302 are outside of the scope of this study but they could be the cosmic forces such as the Sun
303 and other forces acting in our solar system. There are studies proposing the possible
304 reasons [24], [25] and the synthesis analysis combining these reasons together with the GH
305 gases [26] showing very high correlations starting from year 1880.
306

307 In Fig. 4 is also depicted the warming impact of GH gases according to the IPCC. This graph
308 is calculated using the CSP value of 0.5 K/(Wm⁻²) and the radiative forcing (RF) values of
309 GH gases. The temperature change, according to this method, is about 0.2 °C higher than
310 the measured temperature at the end of the period. The error becomes even greater, if the
311 calculation would be started from the year 1750. The RF of GH gases in 2011 was 2.29
312 Wm⁻² [21] and the increase from 2011 to 2015 has been 0.149 Wm⁻² [27]. This means that
313 the temperature increase caused by GH gases would be 0.5 (K/(Wm⁻²)) * 2.44 Wm⁻² = 1.22
314 °C since 1750. It is 44 % higher than 0.85 °C which is the average temperature of the pause
315 period since 2000.
316

317 During the period from 1979 to 2000 the IPCC-model follows very accurately the long-term
318 trend of temperature. Even during this period there is a serious problem in the model that it
319 is based on the positive feedback of water. During this period the real TWP content has a
320 slight downward trend, and therefore it cannot double the warming impacts of GH gases.

321 When the real causes of warming do not increase anymore after 2000, the IPCC model still
 322 shows a strong increasing trend.

323

324 **4. CONTRIBUTIONS OF GREENHOUSE GASES IN GLOBAL WARMING**

325

326 **4.1 The Contributions of Greenhouse Gases in the Greenhouse Effect**

327

328 As summarized in section 1.2, the results of GH gases in the GH effects deviate a lot in the
 329 published research results. Because the lowest values for CO₂ warming effects are
 330 calculated for clear sky conditions, I have carried out a new analysis for calculating the
 331 results for all-sky conditions. The all-sky radiation fluxes and temperatures can be calculated
 332 as a combination of clear and cloudy sky values [28] utilizing the following equation

333

$$334 \quad (1-k) * F_b + k * F_o = F_a \quad (5)$$

335

336 where F_b is the radiation flux of the clear sky, F_o is the radiation flux of the cloudy sky, F_a is
 337 the radiation flux of the all-sky, and k is the all-sky cloud cover factor [15]. In this study the
 338 value of k is 0.66, which means a cloudiness-% of 66 %.

339

340 The published values of average global cloud base and cloud top vary a lot. The results
 341 based on the radiosonde stations are 0.6 km for the base and 9.0 km for the top in 1995
 342 [29]. The same values based on the weather satellite measurements over 20 years' dataset
 343 show the values of 1.6 km and 4.0 km [30]. The result of applying a semi-analytical cloud top
 344 height retrieval algorithm based on an asymptotic solution of the radiative transfer equation
 345 in the oxygen A-band gives the cloud top value of 6 km [31]. This analysis is valid for thick
 346 clouds only.

347

348 In this study the cloud base and top values of 1.6 km and 4.0 km have been used. The
 349 absorption calculations have been carried out by applying the AGA15 climate profile for the
 350 altitude of 120 km. In this connection, the absorption according to the altitude was
 351 calculated, and a technical problem in the Spectral Calculator was noticed. Namely the
 352 absolute absorption change in 1 km altitude without CO₂ was 20.092 Wm⁻², and in the
 353 altitude of 11 km, it was 16.515 Wm⁻². There are two probable reasons for this, which occur
 354 at the same time.

355

356 In the atmospheric paths, the Spectral Calculator [1] divides the path into concentric
 357 spherical shells. The number of shells depends on the path and altitude range. For example,
 358 a path to 120 km altitude is split into 19 shells. The lowest shell is 250 meters thick and the
 359 highest is 10 km thick. In these shells, Spectral Calculator uses mass weighted values of
 360 temperature, pressure, and concentrations. This means that the calculation is more accurate
 361 for low altitude range of 1 km (the minimum for atmospheric paths) than the one of 11km
 362 range. This seems to create an accuracy problem for CO₂, which is a very strong GH gas in
 363 its absorption range from 12 μm to 19 μm. In the range from 14 μm to 16 μm CO₂ alone
 364 could easily absorb all the available infrared radiation emitted by the Earth's surface. In other
 365 words, in the presence of water, the CO₂ effect does not grow after the altitude of 1 km even
 366 though its concentration is practically the same up to the altitude of 80 km. After finding out
 367 this problem, the author has used the value of 20.092 Wm⁻² for the total contribution of CO₂
 368 from the concentration 0 ppm to 400.83 ppm. The author checked that this problem does not
 369 exist for CH₄ and N₂O, which are much weaker absorbers in the present-day atmosphere.

370

371 A very decisive selection is the calculation method. I have calculated the contribution of each
 372 GH gas by removing it from the atmospheric model. One of the most essential features of
 373 our planet is the ocean covers 70 % of our planet's area. They provide humidity into the

374 atmosphere, which has the key role in the GH phenomenon. Therefore, it is a justified
 375 assumption that there is water all the time in the atmosphere.

376

377 The contributions are calculated for the clear sky and they are depicted in Table 4.

378

379

380

Table 4. The warming effects of GH gases in the clear sky conditions.

GH gas	Absorption	Absorption change	Percentage
Total	310.69		
CO ₂	294.25	20.1	14.9
O ₃	303.50	7.2	5.3
CH ₄ & N ₂ O	308.65	2.1	1.5
H ₂ O		105.7	78.3
Total		135.1	100.0

381

382 The total absorption of the clear sky 135.1 Wm⁻² is the difference of the surface emitted
 383 radiation flux 394.10 Wm⁻² and the OLR at the TOA 259 Wm⁻² [15]. These results show
 384 higher contribution for CO₂ (14.9 % versus 11.0 %) than those of the earlier study [6]. The
 385 contribution-% 14.9 is close to the one reported by Schmidt et al. [7] for a single factor
 386 removal process (14.0 %).

387

388 The results for the cloudy sky are summarized in Table 5.

389

390

391

Table 5. The warming effects of GH gases in the cloudy sky conditions.

GH gas	Below clouds 0-1.6 km			Altitude 0-4.0 km		4-120 km	Cloudy sky, total	
	Absor.	Absor. change	%	Absor.	Absor. change	Absor. change	Absor. change	%
Total	289.03	21.66		301.75	22.36	8.94		
CO ₂	257.77	20.09	17.7	287.60	20.09	0.0	20.09	11.9
O ₃	277.64	0.33	0.3	301.02	0.73	6.46	6.79	4.0
CH ₄ & N ₂ O	276.73	1.32	1.1	300.21	1.54	0.51	1.74	1.0
H ₂ O		91.78	80.9		103.80	1.97	93.75	55.3
Clouds		0.0	0.0		0.0	0.0	47.02	27.8
Total		113.44	100		126.2		169.4	100

392

393 The total absorption 169.4 Wm⁻² of the cloudy sky is the difference of the surface emitted
 394 radiation flux 396.20 Wm⁻² and the OLR at the TOA 222.8 Wm⁻² [14]. The absorption fluxes
 395 for the altitudes from the surface to 1.6 km and to 4.0 km, are calculated in the clear sky
 396 conditions. The absorption values for the altitude from 4 km to 120 km are calculated by
 397 subtracting the altitude 0-4 km values from the total absorption 0-120 km. The total GH gas
 398 absorption values can be calculated by summarizing the values of altitudes 0-1.6 km and 4-
 399 120 km. The difference of the total absorption 169.4 Wm⁻² and the GH gases is 47.02 Wm⁻²
 400 and it represents the absorption of clouds. It means that the contribution of clouds would be
 401 27.8 %, which is close to 25 % which was reported by Schmidt et al. [7].

402

403 The absorptions and contributions of GH gases in all-sky conditions are summarized in
 404 Table 6.

405

406
407
408

Table 6. The warming effects of GH gases in the all-sky conditions.

GH gas	All-sky, gross		All-sky, net		
	Absorp. change	%	Absorp. change	%	°C
CO ₂	20.1	12.7	20.1	12.7	4.3
O ₃	6.9	4.4	6.9	4.4	1.5
CH ₄ & N ₂ O	1.8	1.2	1.8	1.2	0.4
H ₂ O	97.8	62.0	127.3	80.7	27.4
Clouds	31.0	19.7	1.6	1.0	0.3
Total	157.7	100	157.7	100	34.0

409

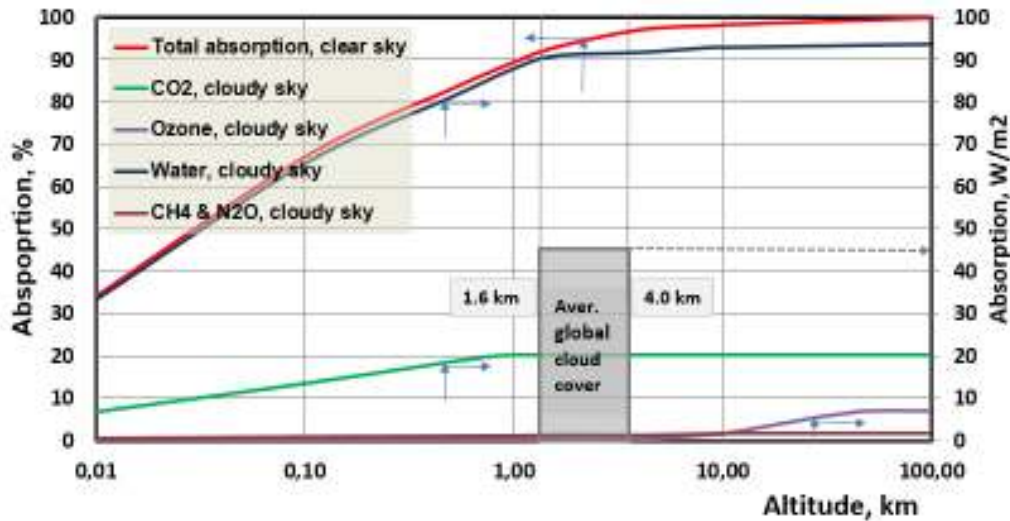
410 The absorption flux values of the all-sky conditions are calculated using equation (5) and the
411 values of clear and cloudy skies in Tables 4 and 5. The total absorption by GH gases and
412 clouds in all-sky is 157.7 Wm⁻². The flux values representing the maximum effects of clouds,
413 have been called *gross values*. Clouds decrease the incoming SW solar radiation but in this
414 calculation basis it has not been considered. We can demonstrate this situation by the
415 greenhouse having glass walls and roofs, and which locates in the polar zone in April.
416 During day-time the incoming solar insolation decreases considerably the need for heating
417 the greenhouse by gas or oil. At night-time, the solar insolation effect decreases and much
418 more heating is needed and it may override the energy-savings at the day-time. If we would
419 calculate the energy savings only during the day-time, we would draw a wrong conclusion
420 that more glass in the walls and in the roof, means more energy savings.

421

422 That is the case of gross effect of clouds in Table 6. Therefore, there is also the *net effect* of
423 clouds included in Table 6. The net effect of clouds is the combination of increased
424 absorption by clouds and therefore increased LW flux downwards and the decreased SW
425 radiation. The most reliable measure of this net effect is the observed surface temperature
426 increase of 0.3 °C between clear sky and all-sky [14]. The increased absorption value of 1.6
427 Wm⁻² is a theoretical absorption increase, which could create this temperature change. The
428 net absorption percentages of GH gases and clouds are calculated from the total absorption
429 of 157.7 Wm⁻². This calculation basis is not univocal for H₂O, because it is calculated by
430 subtracting the total absorption of other GH gases from the total absorption. Anyway, if the
431 contribution-% of H₂O in the clear sky is 78.3 %, and the one of the all-sky is 80.7 %, the
432 conclusion is that this small increase is in the right direction, because the humidity of the all-
433 sky is higher than that of the clear sky. These results are depicted in Fig. 6.

434

435



436
437
438
439
440
441
442
443
444
445
446
447
448
449
450
451
452
453
454
455
456
457
458

Figure 6. The absorption effects of GH gases in the clear and cloudy sky conditions.
The altitude axis is logarithmic.

The graphs in Fig.6 show that the total absorption in 1.6 km is already 93 % of that of 120 km. That is why the GH impacts of all-sky are very close to the values of the clear sky. The absorption effects of O₃ happens mainly in the stratosphere.

4.2 The Relative Strengths

The analysis of the contributions of GH gases in the GH effect is not applicable for the present-day atmosphere. The reason is that the warming impacts are too nonlinear. A separate analysis was carried out to find out the relative strengths by increasing the concentrations by 10 % and calculating the absorption for the altitude of 120 km.

Also in calculating the increased absorption caused by 10 % concentration increase, the CO₂ calculation was carried for the altitude of 1 km only. The other calculations were carried in the altitude of 120 km. The results are shown in Table 7.

Table 7. The increased absorption caused by the 10 % increase of concentration in AGA15 atmosphere. The reference value of the AGA15 absorption is 310.69 Wm⁻². The CO₂ change is based in the altitude of 1 km.

GH gas	Total absorption	Absorption change	Relative strength
H2O	315.129	4.439	11.765
CO2	(310.996)	0.394*	1
O3	310.998	0.308	0.782
N2O	310.745	0.055	0.140
CH4	310.733	0.043	0.109

459
460
461
462
463

In the earlier study the relationship between H₂O:CO₂ was 15.2:1 and now it is 11.8:1. The main reason is in the more accurate calculation method for CO₂ absorption.

464 4. CONCLUSION

465

466 The new updates of Spectral Calculator with HITRAN 2012 and water continuum increases
467 the absorption results of GH gases in the atmosphere only by 0.2 % in comparison to the
468 older versions. This means that the results using the older versions are still applicable.

469

470 The analysis of the absorptions by climate zones approve that the absorption using the
471 single average global atmosphere (AGA) profile has only 0.5 % difference to the sum of five
472 different climate zones of the Earth. This means that the simulation using only one AGA
473 profile is justified. The water content of a climate zone increases as the temperature
474 becomes warmer. If the Earth would follow this humidity behavior, the water feedback would
475 be positive and it would increase the warming impacts of other GH gases by 35 %.

476

477 The analysis of the period from 1979 to 2015 shows that the effects of water and other GH
478 gases cannot explain the temperature trend. The warming impacts of GH gases (water
479 feedback doubles the impacts of other GH gases) according to the IPCC model [21] are 44
480 % higher than the observed temperature in 2015 when compared to the average
481 temperature from 2000 to 2015. The same impacts calculated by Ollila's formula [6] for the
482 radiative forcing of CO₂, shows that the difference varies from 0 to 0.45 °C during this period.
483 The trend analysis shows that there is no water feedback during the three latest solar cycles.
484 The conclusion is that the absolute water content can be kept constant in the long-term
485 climate change analyses.

486

487 The detrended analysis shows very clearly that the short-term (1-2 years) CO₂ changes do
488 not change the short-term absolute humidity values at all - there is no correlation. The culprit
489 for the short-term changes is the ENSO event (El Niño and La Niña), which creates strong
490 changes in the absolute water content. Usually this phenomenon is called positive water
491 feedback but this term can be questioned in the ENSO events. When the temperature of the
492 surface ocean increases, it increases evaporation and it gives rise to the water content in the
493 atmosphere. The atmospheric TPW changes during ENSO events are the essential parts of
494 the whole process and not actually separate feedback processes. The strong short-term
495 global level changes of water amounts explain, why the El Niño and La Niña changes are so
496 strong and why these regional phenomena have global effects after a 2-3 months' delay.

497

498 During the period from 1979 to 2015 there is only one short-term temperature change, which
499 is not due to the ENSO. That is the eruption of Mt. Pinatubo in 1991 leading to the sudden
500 global temperature drop of 0.5 °C, which gradually vanished by 1995. It is interesting to
501 analyze which kind of water feedback can be found if any. Soden et al. [32] reported that
502 there was a water positive feedback applying -0.75 mm TPW peak reduction as to the
503 NVAP-M trend [33] during the eruption. Ollila [34] found that it was impossible to draw any
504 conclusions based on the trend TWP values, because the two datasets had opposite trends
505 [23], [33]. The TPW trend in Fig. 4 is after NCEP/NCAR Reanalysis dataset and there is no
506 trend from 1991 to 1995 meaning no water feedback. Therefore, the conclusion of the
507 constant water content during the long-term temperature changes seems to be justified,
508 because TPW changes happen only during ENSO events. This result supports the climate
509 sensitivity (CS) calculations, where the absolute water amount has been assumed to be
510 constant, and which gives the CS value of 0.6 °C [6].

511

512 At the same time, there is an unknown force or forces, which create long-term temperature
513 changes like the strong warming from 1985 to 2000. These unexplained warming effects
514 vary between from 0 to 0.45 °C as noticed before. They could be cosmic forces. The
515 absolute water amount does not react to the long-term temperature changes (> 11 years).

516

517 The analyses of the GH gas impacts show that the impact of CO₂ is very nonlinear. The
 518 effects of GH gases for the all-sky are: H₂O 79 %, CO₂ 13 %, O₃ 5 %, CH₄ & N₂O 1 % and
 519 cloud 2 %. The cloud effort considers only the temporary (in average from 1 to 10 days)
 520 cloudiness changes of the Earth. The long-term cloudiness change increases still have the
 521 negative impact on the surface temperature (-0.1 °C / cloudiness-%) [15]. These results
 522 mean that the all-sky values are close to clear sky values. The main reason is that the
 523 absorption in the altitude of 1.6 km is already 93 % of the total absorption in the altitude of
 524 120 km. In these analyses the cloud base value has been 1.6 km and the cloud top value 4.0
 525 km.
 526

527 The effects of GH gases show that the warming effect of CO₂ is very nonlinear: in the GH
 528 phenomenon waters strength to CO₂ is 6.2:1, and in the present climate it is 11.8:1. The total
 529 absorption without CO₂ is 285.684 Wm⁻², which is very close to the absorption flux, if there is
 530 only water in the atmosphere: 286.704 Wm⁻². This latter water absorption is possible only, if
 531 the atmosphere can maintain the constant water amount 2.6 prcm of the present
 532 atmosphere. The empirical data shows that this is the case of the relatively small long-term
 533 changes of 0.5 °C. Whether this would happen in the case of the average temperature drop
 534 of 4.3 °C, we have no physical evidence. Anyway, the climate system seems to prefer
 535 maintaining the constant absolute water amount in the atmosphere rather than the constant
 536 relative water amount (positive feedback) or negative feedback, which would mean the
 537 constant greenhouse conditions.
 538
 539

540 REFERENCES

- 541
- 542 1. Gats, Inc. Spectral calculations tool: Available: <http://www.spectralcalc.com/info/help.php>
 543 2015.
 - 544 2. HITRAN, Harvard-Smithsonian Center for Astrophysics, The HITRAN (high-resolution
 545 transmission molecular absorption) data base. Available:
 546 <https://www.cfa.harvard.edu/hitran/>
 - 547 3. Mlawer EJ, Payne VH, Moncet J-L, Delamere JS, Alvarado MJ, and Tobin DC.
 548 Development and recent evaluation of the MT_CKD model of continuum absorption.
 549 Philosophical transactions. Series A, Mathematical, physical, and engineering sciences.
 550 2012;370:Jun 13:2520-56. doi:10.1098/rsta.2011.0295. 2012.
 - 551 4. Michell JFB. The "greenhouse" effect and climate change. Reviews of Geophysics.
 552 1989;27(1):115-139.
 - 553 5. Kiehl JT and Trenberth KE. Earth's annual global mean energy budget. Bulletin of
 554 American Meteorological Society. 2009;90:311-323.
 - 555 6. Ollila A. The potency of carbon dioxide (CO₂) as a greenhouse gas. Development in
 556 Earth Sciences. 2014;2:20-30.
 - 557 7. Schmidt GA, Ruedy RA, Miller RL, Lacis AA. Attribution of the present-day total
 558 greenhouse effect. Journal of Geophysical Research. 2010;115:D20106.
 559 doi:10.1029/2010JDO14287.
 - 560 8. Clough SA, Iacono MJ. Line-by-line calculations of the atmospheric fluxes and cooling
 561 rates 2. Application to carbon dioxide, ozone, methane, nitrous oxide and the
 562 halocarbons. Journal of Geophysical Research. 1995;100:16519-16535.
 - 563 9. Miskolczi FM, Mlynczak MG. The greenhouse effect and spectral decomposition of the
 564 clear-sky terrestrial radiation. Időjaras. 2004;108:209-251.
 - 565 10. Pierrehumbert RT. Infrared radiation and planetary temperature. Physics Today.
 566 2011;64:33-38.
 - 567 11. Ollila A. Analyses of IPCC's warming calculations results. Journal of Chemical, Biological
 568 and Physical Sciences. 2013;3:2912-2930.

- 569 12. Chambers J, Miller A, Morgan R, Officer B, Rayner M, Quirk T. Clearing air on climate.
570 Energy & Environment. 2010;21:632-639.
- 571 13. Ollila A. Dynamics between clear, cloudy and all-sky conditions: cloud forcing effects.
572 Journal of Chemical, Biological and Physical Sciences. 2013;4:557-575.
- 573 14. Zhang Y, Rossow WB, Lacis AA, Oinas V, Mischenko MI. Calculation of radiative fluxes
574 from the surface to top of atmosphere based on ISCCP and other global data sets.:
575 Refinements of the radiative model and the input data. Journal of Geophysical Research.
576 2004:1149-1165.
- 577 15. Ollila A. Earth's energy balance for clear, cloudy and all-sky conditions. Development in
578 Earth Sciences. 2013;1:1-9.
- 579 16. Ollila A, The roles of greenhouse gases in global warming. Energy & Environment.
580 2012;23:781-799.
- 581 17. Ollila A. Clear sky absorption of solar radiation by the average global atmosphere.
582 Journal of Earth Sciences and Geotechnical Engineering. 2015;5:19-34.
- 583 18. IPCC. Climate response to radiative forcing. IPCC Fourth Assessment Report (AR4),
584 The Physical Science Basis, Contribution of Working Group I to the Fourth Assessment
585 Report of the Intergovernmental Panel on Climate Change, Cambridge University Press,
586 Cambridge. 2007
- 587 19. Miskolczi F. The stable stationary value of the earth's global average atmospheric
588 Planck-weighted greenhouse-gas optical thickness. Energy & Environment.
589 2010;21:243-262.
- 590 20. NOAA. Global CO₂ data base. Available:
591 ftp://aftp.cmdl.noaa.gov/products/trends/co2/co2_mm
- 592 21. IPCC. The Physical Science Basis. Working Group I Contribution to the IPCC Fifth
593 Assessment Report of the Intergovernmental Panel on Climate Change, Cambridge
594 University Press, Cambridge. 2013.
- 595 22. UAH MSU dataset. Available:
596 http://vortex.nsstc.uah.edu/data/msu/v6.0beta/tlt/uahncdc_lt_6.0beta5.txt
- 597 23. NVAP dataset. NCEP/NCAR Reanalysis. Available:
598 <http://www.esrl.noaa.gov/psd/data/timeseries/>
- 599 24. Ermakov V, Okhlopov V, Stozhkov Y, Yu I. Influence of cosmic rays and cosmic dust on
600 the atmosphere and Earth's climate. Bulletin of Russian Academy of Sciences: Physics.
601 2009;73:434-436.
- 602 25. Scafetta N. Empirical evidence for a celestial origin of the climate oscillations and its
603 implications. Journal of Atmospheric and Solar-Terrestrial Physics. 2010;72:951-970.
- 604 26. Ollila A. Cosmic theories and greenhouse gases as explanations of global warming.
605 Journal of Earth Sciences and Geotechnical Engineering. 2015;5:27-43.
- 606 27. AGGI. The NOAA annual greenhouse index (AGGI). Available:
607 <http://www.esrl.noaa.gov/gmd/aggi/aggi.html>
- 608 28. Bellouin n, Boucher O, Haywood J, Shekar Reddy M. Global estimate of aerosol direct
609 radiative forcing from satellite measurement. Nature. 2003;438:1138-1141.
- 610 29. Chernykh IV, Alduchov OA, Eskridge RE. Trends in Low and High Cloud Boundaries
611 and Errors in Height Determination of Cloud Boundaries. Bulletin of the American
612 Meteorological Society. 2001;82:1941-1947.
- 613 30. Wang J, Rossow WB, Zhang Y. Cloud vertical structure and its variations from a 20-yr
614 global rawinsonde dataset. Journal of Climate. 2000;13:3041-3056.
- 615 31. Kokhanovsky AA, Rozanov VV, Lotz W, Bovensmann H, Burrows JP. Global cloud top
616 height and thermodynamic phase distributions as obtained by SCIAMACHY on
617 ENVISAT. International Journal of Remote Sensing.2011;28:836-844.
- 618 32. Soden BJ, Wetherald RT, Stenchikov GL, Robock A. Global cooling after the eruption of
619 Mount Pinatubo: A test of climate feedback by water vapor. Science. 2002; 296:727-730.
-

- 620 33. Vonder Haar TH, Bytheway JL, Fortsyth JM. Weather and climate analyses using
621 improved global water vapor observations. *Geophysical Research Letters*.
622 2012;39:L16802.
- 623 34. Ollila A. Climate sensitivity parameter in the test of the Mount Pinatubo eruption.
624 *Physical Science International Journal*. 2016;9(4):1-14.
-